

Ultrasonic and Brillouin scattering measurements of the elastic constants of SrFCI

This article has been downloaded from IOPscience. Please scroll down to see the full text article.

1994 J. Phys.: Condens. Matter 6 10407

(<http://iopscience.iop.org/0953-8984/6/47/023>)

View [the table of contents for this issue](#), or go to the [journal homepage](#) for more

Download details:

IP Address: 171.66.16.151

The article was downloaded on 12/05/2010 at 21:12

Please note that [terms and conditions apply](#).

Ultrasonic and Brillouin scattering measurements of the elastic constants of SrFCl

M Fischer†, A Polian‡ and M Sieskind§

† Département de Recherches Physiques (Unité associée au CNRS 71), Université Pierre et Marie Curie, T 22, 4 place Jussieu, 75252 Paris Cédex 05, France

‡ Physique des Milieux condensés (Unité associée au CNRS 782), Université Pierre et Marie Curie, T 13, 4 place Jussieu, 75252 Paris Cédex 05, France

§ CNRS Laboratoire Phase, 23 rue du Loess, 67037 Strasbourg Cédex, France

Received 3 March 1994, in final form 27 July 1994

Abstract. The six second-order elastic constants of SrFCl, which is a crystal belonging to the matlockite family, have been measured using ultrasonic and Brillouin scattering techniques. The linear and volume compressibilities are deduced and compared with those of the isostructural compound BaFCl. An elastic Debye temperature Θ_{el} is calculated and compared with other experimental (calorimetric) and theoretical (shell model) determinations. The elastic constants of SrFCl and BaFCl are compared with those of BaF₂ and SrF₂, because the matlockite structure of MF_x crystals can be derived from the fluorine structure of MF₂ crystals. Finally, these constants are also compared with those deduced from shell model calculation.

1. Introduction

Fluorohalides with the matlockite (PbFCl) structure are compounds whose technological interest is exemplified in their use in the image plate x-ray detectors. They are layer compounds whose two-dimensionality is more or less pronounced, depending on the composition of the crystal.

In our previous paper [1], we reported on the elastic properties of BaFCl under ambient conditions and compared the experimental results with elastic constants calculations using a shell model (SM) [2].

In the present paper, we report results obtained by ultrasonics and Brillouin scattering on the elastic properties of the isostructural compound SrFCl.

Like the matlockite crystals, SrFCl is tetragonal and belongs to the D_{4h}^7 space group. It is characterized by six independent elastic constants C_{11} , C_{33} , C_{44} , C_{66} , C_{12} and C_{13} . C_{33} and C_{44} determine the velocities of phonons propagating parallel to the C_4 axis and C_{11} , C_{12} , C_{44} and C_{66} those of the phonons propagating perpendicular to it. C_{13} appears in the expression for the velocity to intermediate directions. The six second-order elastic constants have been measured using ultrasonic and/or Brillouin scattering techniques. The linear and volume compressibilities are computed and an elastic Debye temperature Θ_{el} is calculated and compared with other theoretical and experimental determinations. Finally, the elastic constants are compared with those of BaFCl [1] and with those deduced from SM calculations [2]. They are also compared with those of BaF₂ and SrF₂ because the structure of the matlockite-type crystals MF_x can be derived from the fluorine-type crystals MF₂.

2. Experiments

2.1. Crystal growth

Single crystals were grown by slowly cooling a molten mixture of carefully dehydrated SrCl_2 and SrF_2 in a dry argon atmosphere. Details of the growth procedure have been published elsewhere [3]. Typical crystal dimensions are 4 mm \times 5 mm \times 8 mm. These samples are clear and colourless single crystals. Crystals orientations were identified by Laue x-ray diffraction techniques.

2.2. Ultrasonic measurements

The samples used in the present experiments were large polished parallelepipeds with various dimensions ranging from 3.9 to 8.4 mm. The parallelism of flat opposite faces was better than 1° .

Table 1. Ultrasonic wave velocities for various propagation and polarization directions.

Propagation direction	Polarization direction	Velocity	Ultrasonic velocity (m s ⁻¹)
[010]	[010]	$\sqrt{C_{11}/\rho}$	4852 \pm 50
[001]	[001]	$\sqrt{C_{33}/\rho}$	4392 \pm 6
[1 $\bar{1}$ 0]	[001]	$\sqrt{C_{44}/\rho}$	2686 \pm 9
[010]	[001]	$\sqrt{C_{66}/\rho}$	2812 \pm 9
[110]	[1 $\bar{1}$ 0]	$\sqrt{(C_{11} - C_{12})/\rho}$	2842 \pm 100
[110]	[110]	$\sqrt{(C_{11} + C_{12} + 2C_{66})/2\rho}$	4840 \pm 64

Four directions of ultrasonic wave propagation with different polarization directions were used to determine C_{11} , C_{33} , C_{44} , C_{66} and C_{12} (table 1). The transit time of an ultrasonic pulse through the sample was measured using the phase quadrature detection method [4]. Then, the wave propagation velocities, the elastic moduli ρV^2 and the elastic constants were calculated from knowledge of this transit time, the path length and the density $\rho = 3.985 \pm 0.001$ g cm⁻³ (see tables 1 and 3). The errors in the determination of the sample length and the density are negligible in comparison with the errors from the transit time measurement. So, the errors in the velocity measurements are essentially due to the latter. The accuracy of the transit time depends on the signal phase quality. The uncertainties in tables 1 and 3 indicate only the consistency of measurements repeated on several samples using two or three successive echoes.

2.3. Brillouin scattering measurements

The samples (large polished parallelepipeds) used in these experiments had faces perpendicular to the [010], [001], [10 $\bar{1}$], [1 $\bar{1}$ 0] and [110] directions. In addition, small as-grown platelets of 5 mm \times 5 mm \times 0.5 mm were used with the smallest dimension along the [001] direction.

The piezoelectrically scanned Fabry-Pérot interferometer used was either a five-pass or a six-pass tandem. The excitation light ($\lambda = 514.5$ nm) was produced with an argon laser of power about 50 mW. Different free spectral ranges of the Fabry-Pérot interferometer were used in the range of 1.5 cm⁻¹. Various scattering geometries were used. The sound velocity

(phonon velocity) can be deduced from the measurement of the Brillouin wavenumber shift $\Delta\sigma$ if the refractive index of the crystal is known and is given by the following relation:

$$V = \frac{\lambda_0 C \Delta\sigma}{2n \sin(\varphi/2)} \quad (2.1)$$

with λ_0 the wavelength of the laser light in vacuum, C the velocity of the light in vacuum and φ the angle between the incident and scattered photons. The ordinary refractive index n_o and the extraordinary refractive index n_e were measured using the Abbe refractometer technique for $\lambda_0 = 514.5$ nm, and the following values were obtained: $n_o = 1.645 \pm 0.001$ and $n_e = 1.626 \pm 0.001$.

Table 2. Brillouin scattering measurements of acoustic velocities for various scattering configurations. X, Y, Z, T, U, V and W indicate the [100], {010}, [001], [101], [10 $\bar{1}$], [1 $\bar{1}$ 0] and [110] directions, respectively. The configuration $A(B)D$ indicates that the incident and scattered light are along the A and D directions, respectively, with the incident polarization vector parallel to B . The polarization of scattered light is not analysed.

Configuration	Velocity	Value from Brillouin measurement (m s ⁻¹)
$Y(X)\bar{Y}$	$\sqrt{C_{11}/\rho}$	4785 \pm 5
$Z(V)\bar{Z}$	$\sqrt{C_{33}/\rho}$	4397 \pm 14
$V(W)\bar{W}$	$\sqrt{(C_{11} + C_{12} + 2C_{66})/2\rho}$	4779 \pm 47
$U(T)\bar{U}$	V_+	4799 \pm 10
	V_-	2336 \pm 5
	V_T (45°)	2707 \pm 5

The results of the velocity measurements with various scattering configurations inside the large parallelepipedic samples are given in table 2. The uncertainties in the values of the velocities determined by Brillouin scattering do not take into account the accuracy of the refractive index measurements and indicate the consistency of the Stokes and anti-Stokes measurements. When the wavevector of the phonon lies in the (101) plane, the velocity V_+ of a quasi-longitudinal phonon, the velocity V_- of a quasi-transverse phonon and the velocity V_T of a transverse phonon can be determined. These velocities are related to the elastic constants combinations which involve the constants C_{11} , C_{33} , C_{44} , and C_{13} and are given by

$$V_{\pm} = \frac{1}{\sqrt{2\rho}} \left[(\Gamma_{11} + \Gamma_{33}) \pm \sqrt{(\Gamma_{33} - \Gamma_{11})^2 + 4\Gamma_{13}^2} \right]^{1/2} \quad (2.2)$$

$$V_T = \frac{1}{\sqrt{\rho}} (\Gamma_{22})^{1/2} \quad (2.3)$$

where

$$\Gamma_{11} = C_{11} \sin^2 \theta + C_{44} \cos^2 \theta \quad (2.4)$$

$$\Gamma_{22} = C_{66} \sin^2 \theta + C_{44} \cos^2 \theta \quad (2.5)$$

$$\Gamma_{33} = C_{44} \sin^2 \theta + C_{33} \cos^2 \theta \quad (2.6)$$

$$\Gamma_{13} = (C_{13} + C_{44}) \sin \theta \cos \theta \quad (2.7)$$

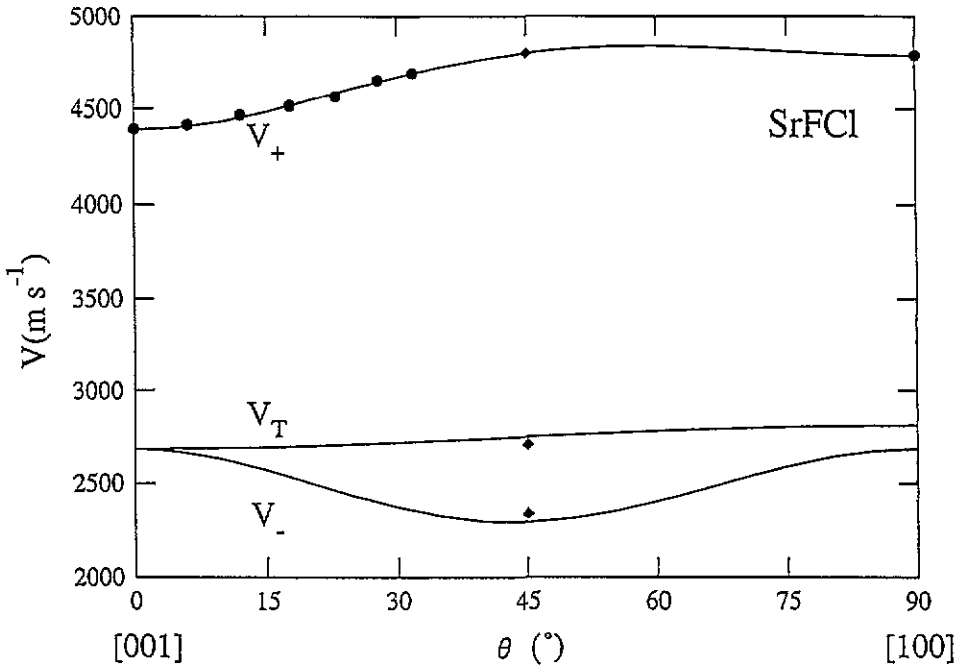


Figure 1. Brillouin scattering measurements of a quasi-longitudinal acoustic wave velocity versus the angle between the phonon propagation direction and the [001] direction of the as-grown platelet: \blacklozenge , obtained with the scattering configuration $U(T.)\bar{U}$ inside a parallelepipedic sample; —, calculated from equations (2.2) and (2.3).

and θ is the angle between the phonon propagation direction and the [001] direction of the crystal.

The results of the Brillouin scattering inside the small as-grown platelets for different θ -values are shown in figure 1. Only one Brillouin peak relative to a quasi-longitudinal phonon was detected (full circles in figure 1). The three points (full diamonds) at $\theta = 45^\circ$ were obtained with the scattering configuration $U(T.)\bar{U}$ (see table 2 caption) inside a large parallelepipedic sample. In this configuration, C_{44} and C_{13} are deduced from equation (2.2) with $\theta = 45^\circ$ and are given by the following relations:

$$C_{44} = \rho V_+^2 + \rho V_-^2 - \frac{C_{11} + C_{33}}{2} \quad (2.8)$$

$$C_{13} = -C_{44} + [(\rho V_+^2 - \rho V_-^2)^2 - \frac{1}{4}(C_{11} - C_{33})^2]^{1/2}. \quad (2.9)$$

With the selected values of C_{11} and C_{33} (see table 3), C_{44} and then C_{13} are calculated (see Brillouin values in table 3). C_{66} is deduced from this value of C_{44} and the velocity measurement of the pure shear acoustic mode: $V_T(45^\circ) = \sqrt{(C_{44} + C_{66})/2\rho}$. Finally, C_{12} is calculated from the value of the velocity of the longitudinal mode in the [110] direction ($\sqrt{(C_{11} + C_{12} + 2C_{66})/2\rho}$) using the selected values of C_{11} and C_{66} (table 3).

The experimental points relative to the quasi-longitudinal phonon in figure 1 were fitted by equation (2.2) which defines V_+ as a function of θ , using the selected values of C_{11} , C_{33} and C_{44} , C_{13} being the only adjustable parameter. The best fit was obtained with $C_{13} = 41.8$ GPa. The selected value of C_{13} was calculated as a weighted mean value between this last value of C_{13} and the value determined from the large sample (table 3).

Table 3. Elastic constants of SrFCl. $\Delta C/C$ is equal to the difference between the calculated and the selected values divided by the selected value.

Elastic constant	Ultrasound value	Brillouin value	Selected value	Calculated value	$\Delta C/C$ %
C_{11} (GPa)	93.8 ± 2	91.2 ± 0.2	91.2 ± 0.2	106.1	15
C_{33} (GPa)	76.8 ± 0.2	77.0 ± 0.5	76.9 ± 0.3	82.9	7
C_{44} (GPa)	28.7 ± 0.2	29.5 ± 1.3	28.7 ± 0.2	30.6	6
C_{13} (GPa)		40.2 ± 1.4	41.6 ± 1.4	45.8	10
C_{66} (GPa)	31.5 ± 0.2	30.9 ± 0.8	31.5 ± 0.2	37.9	18
C_{12} (GPa)	29.6 ± 2.6	29.0 ± 1.8	29.3 ± 2.2	33.2	12

The full curves in figure 1 are calculated from equations (2.2) and (2.3).

2.4. Results

Table 3 is a summary of the elastic constants obtained from the two techniques. When the accuracies of the ultrasonic and Brillouin scattering measurements are of the same order of magnitude, the selected value of the elastic constant is the mean value (or the weighted mean value) of the two measurements. On the contrary, when the accuracies of the two measurements are very different, we propose the value with the best accuracy as the selected value. The agreement is generally good between the ultrasonic and the Brillouin scattering measurements and particularly for C_{33} (2 per thousand). The selected values are also compared with the theoretical values calculated from a SM [2]. Surprisingly, one of the largest differences between experimental and calculated values is for C_{11} (15%). The discrepancy is even larger for C_{66} (18%) but it is less significant because C_{66} is not obtained by a direct measurement, in contrast with C_{11} .

2.5. Compressibilities

The linear compressibility χ_{\parallel} along a direction parallel to the C_4 axis and the linear compressibility χ_{\perp} along a perpendicular direction to this axis are related to the elastic constants by

$$\chi_{\parallel} = \frac{C_{11} + C_{12} - 2C_{13}}{C_{33}(C_{11} + 2C_{12}) - 2C_{13}^2} \quad (2.10)$$

$$\chi_{\perp} = \frac{C_{33} - C_{13}}{C_{33}(C_{11} + 2C_{12}) - 2C_{13}^2} \quad (2.11)$$

The bulk compressibility is given by $\chi = \chi_{\parallel} + 2\chi_{\perp}$. For SrFCl, the values of the compressibilities are

$$\chi_{\parallel} = 4.6 \times 10^{-3} \text{ GPa}^{-1} \quad \chi_{\perp} = 4.3 \times 10^{-3} \text{ GPa}^{-1} \quad \chi = 13.2 \times 10^{-3} \text{ GPa}^{-1}.$$

If we compare the values of $\chi_{\perp}/\chi_{\parallel}$ in this crystal with those obtained in the isostructural compound BaFCl which is another compound of the matlockite family, we obtain

$$\left(\frac{\chi_{\perp}}{\chi_{\parallel}}\right)_{\text{SrFCl}} = 0.93 > n \left(\frac{\chi_{\perp}}{\chi_{\parallel}}\right)_{\text{BaFCl}} = 0.88.$$

The linear compressibilities are more isotropic in SrFCl than in BaFCl. For SrFCl the ratio $\chi_{\parallel}/\chi_{\perp}$ is determined not only by the value of C_{33}/C_{11} (0.84 in SrFCl; 0.88 in BaFCl) but also by the difference $C_{13} - C_{12}$ which is equal to 12.3 GPa (the difference is only 3.6 GPa in BaFCl).

Table 4. Averaged acoustic wave velocity \bar{V}_m and Debye temperatures.

	\bar{V}_m (m s ⁻¹)	Θ_{cl}^{VRHG} (K)	Θ_{cl}^{HB} (K)	Θ_{cal} (K)
Measured		322	317	305
Calculated	2.92×10^3	341		593.3

Table 5. Elastic constants of BaF₂, SrF₂, BaFCl and SrFCl.

	BaF ₂	SrF ₂	BaFCl		SrFCl	
			Experimental	Calculated	Experimental	Calculated
C_{11} (GPa)	98	124.6	75.9	90.8	91.2	106.1
C_{33} (GPa)	98	124.6	65.7	60	76.9	82.9
C_{44} (GPa)	25.4	31.87	20.38	24.3	28.7	30.6
C_{13} (GPa)	44.8	44.63	31.9	41.6	41.6	45.8
C_{66} (GPa)	25.4	31.87	23.8	33.2	31.5	37.9
C_{12} (GPa)	44.8	44.63	28.3	26.7	29.3	33.2

2.6. Debye temperature

As in the case of BaFCl, let us compare the Debye temperature Θ_{cal} obtained by calorimetric measurements with the Debye temperature deduced from the elastic constants Θ_{el} or calculated using the SM.

The Debye temperature Θ_{cal} was obtained by calorimetric measurements at a very low temperature [5]:

$$\Theta_{cal} = 305 \text{ K.}$$

From the measurements of the elastic constants at room temperature, the Voigt–Reuss–Hill–Gilvarny (VRHG) approximation [6] gives the Debye temperature value

$$\Theta_{el}^{VRHG} = 322 \text{ K}$$

and the method of Houston and Betts [7] a Debye temperature value of

$$\Theta_{el}^{HB} = 317 \text{ K.}$$

The agreement between Θ_{cal} and the two values for Θ_{el} is of the order of 5%.

From elastic constants calculated by Balasubramanian *et al* [8] and using the VRHG approximation a theoretical value of the Debye temperature $\Theta_{el}(SM)$ can be calculated:

$$\Theta_{el}(SM) = 341 \text{ K.}$$

This value is in better agreement with the experimental values than the value computed by Balasubramanian *et al*, $\Theta_{cal}(SM) = 593.3 \text{ K}$, probably as a result of computational error.

The results of the different Debye temperatures are summarized in table 4.

2.7. Comparison between SrFCl and BaFCl and between BaF₂ and SrF₂

As in BaFCl, the elastic constants of SrFCl in table 5 can be classified into two groups: a ‘longitudinal’ group L with C_{11} and C_{33} and with the same hierarchy $C_{11} > C_{33}$; a ‘transverse group’ with C_{44} , C_{66} , C_{12} and C_{13} . All the elastic constants are larger in SrFCl than their counterparts in BaFCl (same situation for BaF₂ and SrF₂). This can be at least partly explained by the shorter interatomic distances in SrFCl and SrF₂ compared with the same distances in BaFCl and BaF₂ ([1] table 4).

Table 6. Measurements of the discrepancy from the acoustic isotropy for BaFCl and SrFCl.

	C_{33}/C_{11}	C_{44}/C_{66}	$C_{44}/[(C_{11} - C_{12})/2]$
BaFCl	0.88	0.87	0.85
SrFCl	0.84	0.95	0.93

It is interesting to measure the discrepancy from acoustic isotropy and to compare from this point of view the behaviours of SrFCl and BaFCl. For this purpose, table 6 leads to interesting comments. For an acoustic isotropic medium,

$$\frac{C_{33}}{C_{11}} = \frac{C_{44}}{C_{66}} = \frac{C_{44}}{(C_{11} - C_{12})/2} = \frac{C_{12}}{C_{13}} = 1. \quad (2.12)$$

Following these criteria, BaFCl shows the same discrepancy with acoustic isotropy if we consider either the longitudinal or the transverse modes, in different directions of the crystal. The situation is more contrasted for SrFCl, this crystal being more isotropic than BaFCl for the transverse waves and less isotropic for the other modes of vibration. Because of the large uncertainties in the values of C_{12} and C_{13} , the ratio C_{12}/C_{13} is not reported in table 6.

3. Conclusion

The measurement of the sound velocities of SrFCl by the ultrasonic and Brillouin scattering techniques gives the whole set of the six elastic constants. The agreement is generally good between the results obtained by these two techniques. These constants are compared with those of BaFCl. Both crystals have similar elastic behaviours. However, BaFCl shows an acoustic anisotropy for longitudinal and transverse modes when SrFCl is more isotropic for the transverse waves and less isotropic for the other modes.

It should be noted that the elastic constants predicted by the SM model are quite close to the experimental values although the hypothesis on force constants originally made with the model is relatively rough.

Acknowledgments

The authors wish to thank Mrs N Lenain (Département de Recherche, Physiques) for her technical assistance in the index of refraction measurements and in the orientation and polishing of the crystals.

References

- [1] Fischer M, Sieskind M, Poljan A and Lhamar A 1993 *J. Phys.: Condens. Matter* **5** 2749
Three errors must be corrected in this reference. Equations (2.3), (2.5) and (3.1) must be replaced by equations (2.2), (2.8) and (2.9), respectively, of the present paper
- [2] Balasubramanian K R, Haridasan T M and Krishnamurthy N 1979 *Chem. Phys. Lett.* **67** 530
- [3] Sieskind M, Ayadi M and Zachman G 1986 *Phys. Status Solidi b* **136** 489
- [4] Wallace P M and Garland C W 1986 *Rev. Sci. Instrum.* **57** 3085
- [5] Sieskind M, Dossmann Y, Kuentzler R and Lambour J P 1994 *J. Phys.: Condens. Matter* submitted
- [6] Kieffer S W 1979 *Rev. Geophys. Space Phys.* **17** 1
- [7] Betts D D, Bhatia A B and Horton G K 1956 *Phys. Rev.* **104** 129
- [8] Balasubramanian K R, Haridasan T M and Krishnamurthy N 1981 *J. Phys. Chem. Solids* **42** 667